Journal of Sound and Vibration (1997) **205**(2), 223–234

THE USE OF CONTROL TO ELIMINATE SUBHARMONIC AND CHAOTIC IMPACTING MOTIONS OF A DRIVEN BEAM

S. R. Bishop

Centre for Nonlinear Dynamics and its Applications, University College London, Gower Street, London WC1E 6BT, England

AND

D. Xu

Centre for Computational Mechanics, National University of Singapore, Singapore 119260

(*Received* 23 *August* 1996, *and in final form* 12 *March* 1997)

Results of a numerical investigation are presented of the behaviour of a mathematical model which approximates the response of a thin metal strip, or beam, held vertically and clamped at its base, which is driven to impact against a motion limiting constraint. Previous theoretical analyses, in conjunction with numerical studies, have highlighted the complicated dynamics that the system exhibits following a single or series of grazing bifurcations. Under certain conditions subharmonic solutions and chaotic impacting motions are unavoidable. These solutions, which involve several impacts per orbital period introducing relatively large impact velocities, have been viewed experimentally. Meanwhile research into the control of chaos, in which unstable orbits embedded within chaotic motions are stabilized, has advanced over recent years. New control methods have been developed and experimentally implemented. The present work brings these two fields together for the first time. Numerical evidence is given for the use of control to eliminate complicated motions by tracking lower periodic solutions. The stabilized motions near the grazing incidence have lower impact velocities than the naturally existing stable solutions leading to a significant reduction of the impact force which may have significant engineering relevance.

1. INTRODUCTION

The study of systems which include impact dates back some considerable time with significant advances made by researchers in the former Soviet Union and Eastern Block countries, usually under the title of vibro-impact systems [1]. Typically written in Russian, this research has been brought to wider attention through further works [2–4] and others. Interest in driven systems which incorporate impacts was rekindled through the discovery of chaotic motions [5–8] and the need to solve practical problems in rattling gears [9], impact print hammers [10], heat exchanger tubes [11, 12], vibration absorbers [13], high speed machinery with clearance connections [14], the articulated mooring tower [15], and more [16].

In many of these studies low dimensional mathematical models were proposed which adequately modelled much of the qualitative behaviour of a physical system with particular emphasis on the classification of bifurcational events. This approach was continued with both experiments [17, 18] and numerical evidence used to verify theoretical

0022–460X/97/320223 + 12 $25.00/0/sv971036

predictions [19, 20] (also see the theoretical approach to motions of a rocking block [21]). A significant advance was made by Nordmark [22] who proposed a two dimensional mapping which characterised the behaviour of a simple impacting system close to the point where impacting first begins. This latter article has in turn sparked off considerable interest with regards to iterative maps with square root singularities. Specifically, period-adding bifurcations were noted in numerical [23] and experimental [24] investigations.

Impacts, particularly those with high velocities, often lead to excessive loads or wear, unacceptable noise, or give rise to resonance phenomena such as rattling and chattering [20]. The cost of any resulting failure, and subsequent environmental ramifications impose considerable restraints on designers trying to avoid or reduce such responses. In this paper a particular physical system is considered for which there is already detailed information [25] and yet the approach will be valid for the whole class of impact oscillators. The purpose of the research is to evaluate the use of a control strategy, based on the stabilisation of unstable orbits, which limits both the number of impacts and the force exchanged on impact. The proposed control method [26] is borrowed from research into the control of chaos stimulated by the work of Ott, Grebogi and Yorke [27]. A scheme for tracking the stabilized solution is established as a parameter is varied [28]. It is shown here, for the first time numerical evidence that the two topics of impacting systems and control of chaos can be combined to improve the system response. To date, this success has been achieved only numerically but the fact that control of chaos has been achieved experimentally in other mechanical systems [29] gives rise to the hope that these results will be reproducible in a physical system such as the vibrating beam used here.

2. PHYSICAL SYSTEM AND MATHEMATICAL MODEL

The physical system under consideration consists of a thin metal strip, or beam, which is clamped in a vertical position with the upper end free to vibrate under the influence of a periodic driving force [18, 25]. When a motion-limiting constraint (e.g., a rigid stop) is introduced, for sufficiently large amplitude of oscillations, impacts will occur as the beam makes contact with the constraint. Idealized elastic collisions instantaneously change the direction of the velocity introducing discontinuity into the system [22]. Such a set-up will display many of complicated features common to other non-linear dynamical systems but, of particular interest, the impact introduces features not seen in smooth counterparts [22, 23].

This driven beam is a simple mechanical system originally devised specifically to investigate the impacting process. The beam is stiff thereby, allowing torsional motions to be ignored. The excitation frequency is chosen to be close to the natural frequency so that vibrations in the fundamental mode by far exceed the beam's response in other modes [25]. Thus the beam's displacement x for present purposes, can be adequately modelled by a (scaled) single degree of freedom linear oscillator

$$\ddot{x} + c\dot{x} + x = f\cos\omega t \tag{1a}$$

with a motion constraint on the rigid stop where a coefficient of restitution rule is applied:

$$x = 1, \qquad \dot{x}_+ = -r\dot{x}_-, \qquad 0 < r < 1. \tag{1b}$$

The parameters c, f and ω are dimensionless damping, forcing magnitude and forcing frequency, and $x = 1$ refers to the position of the rigid stop. When the amplitude of oscillation reaches the rigid stop, an impact occurs such that the velocity $\dot{x}_-$ (before the impact) is immediately altered to the velocity $\dot{x}_+$ (after the impact) with a restitution of the velocity defined by the coefficient r. The model (1), to some extent, has successfully been used to approximate the response of an experimental apparatus of an impacting beam [18, 25], and also studied both theoretically and numerically by Foale and Bishop [17, 19].

It should be noted that, in order to match the occurrence of bifurcations which bound the motions, a reduced value for the coefficient of restitution of $r = 0{\cdot}2$ was applied rather than an expected value of $r \approx 0{\cdot}7$ in these earlier studies [18, 25]. This requirement appears to indicate that during impact energy is lost to, among others things, higher modes. A different choice for the value of r (and indeed a more complex, higher order model) would merely shift the behaviour in parameter space; it should also be borne in mind that similar behaviour has been noted experimentally [24]; therefore in line with these earlier studies, here the value is fixed at $r = 0{\cdot}2$. Further discussion as regards modelling, and improvements to the simple description used here, have been carried out by Van der Vorst *et al*. [30] analyzing the response of a beam via a multi-degree of freedom model. In their work a continuous Hertz type model (also see reference [31]) was selected for the impact process in conjunction with a finite element method after a component mode synthesis analysis to reduce the dimension of the system. Such a model, while more accurate, is thought not to be necessary here to explain the control strategy.

3. GRAZING BIFURCATIONS

When the system evolves from a non-impacting motion towards the stop as a result of a variation in a parameter (e.g., the forcing frequency is used here while others have used clearance between the beam and the stop [4, 32]) a notional zero velocity impact is approached. At this point the system may jump discontinuously (via a bifuration of the supercritical type) into a motion which might be periodic (of period-1 or more typically of longer period involving multiple impacts) or chaotic depending upon other system parameters [20, 22, 33]. A change in the state of the system has occurred: the so-called grazing bifurcation. For further variation of the driving frequency large numbers of unstable, multiple impact periodic orbits exist with windows of stable period-adding solutions. The response following the grazing bifurcation for the Nordmark map [21] was classified by Chin *et al*. [23] which, for the problem at hand, basically equates to three different scenarios for the impact oscillator: I, high r—system jumps directly to chaos with few periodic windows and ultimately chaos; II, intermediate r—windows of chaos and periodic behaviour alternate with reverse period-adding; III, low r—periodic windows effectively overlapping. In a careful experiment Weger *et al*. [24] viewed some of this bifurcational structure and associated the response with a Nordmark map equivalent to $r = 0{\cdot}2$. The existence of large numbers of unstable orbits after the supercritical bifurcation can be numerically verified for the system (1) but have been more rigorously discussed in the work of Budd and co-workers [20, 32, 33], through the behaviour of a similar system and the approximating maps, where the existence of various impacting solutions are mathematically proved. Of particular note is the scaling of the largest Liapunov exponent as the bifurcation is approached [34].

In the case of the beam in question some of these solutions may be seen as undesirable behaviour. Furthermore, immediately after the grazing bifurcation the response (for certain levels of forcing amplitude and certainly for different values of the coefficient of restitution) is extremely sensitive to further variations in the frequency so that prediction of the number of impacts and the impact force becomes (effectively) impossible unless a fine scale numerical analysis is performed.

The global dynamics of the system (1) in the (ω, f) parameter space was initially studied by Thompson *et al*. [18; also see 25] both theoretically and experimentally. Here particular interest is in the parameter regime just after the lower grazing bifurcation which leads to complicated impacting motions. Notwithstanding the previous remarks regarding the inadequacy of this simple model, as an example, the parameters used in this present numerical study are taken as representative of a real beam. A bifurcation diagram is shown in Figure 1 with the fixed parameters $f = 0{\cdot}26$, $c = 0{\cdot}1$, $r = 0{\cdot}2$ and a variation of the forcing frequency ω from 0·8 to 1·3. The vertical co-ordinate of Figure 1 represents the maximum displacement $|x_{max}|$ of oscillations from the original equilibrium point ($x = 0$). The value of $|x_{max}|$ is the maximum absolute value of the displacement during a single forcing period (once transients have decayed) which is then plotted over several periods to allow subharmonic solutions to be recognised. Figure 1 thus shows the overall behaviour of the system (1) or resonance response diagram. Within the range of $\omega \approx 0{\cdot}8$–$0{\cdot}86885$, the system undergoes a period-1, non-impacting motion (NI-P1). The oscillator impacts the rigid stop with zero velocity at the critical value of $\omega_c \approx 0{\cdot}86885$ (the grazing point G corresponding to $x = 1$), After the grazing impact, a series of further bifurcations occur (some of which are additional grazing bifurcations [20, 22, 29]) producing windows of subharmonic orbits of increasing period and chaotic impacting motions (P&C) in the range of $\omega \approx 0{\cdot}86885$–$0{\cdot}94$. Subsequently, following a period doubling bifurcation [25] the system exhibits a simple period-1 motion with one impact per period (P1) which loses stability due to a saddle–node bifurcation (denoted by SN at the value of $\omega \approx 1{\cdot}21$). After the saddle-node bifurcation as the forcing frequency ω increases, the system settles onto the non-impacting period-1 (NI-P1) motion once again. On the other hand, if the value of ω decreases, say from the value of $\omega = 1{\cdot}3$, then the NI-P1 motion continues until at the value of $\omega \approx 1{\cdot}11$ when the oscillator hits the rigid stop resulting in a jump to the impacting period-1 P1 motion. This jump is associated with another grazing bifurcation but here of a saddle–node or fold type [19].

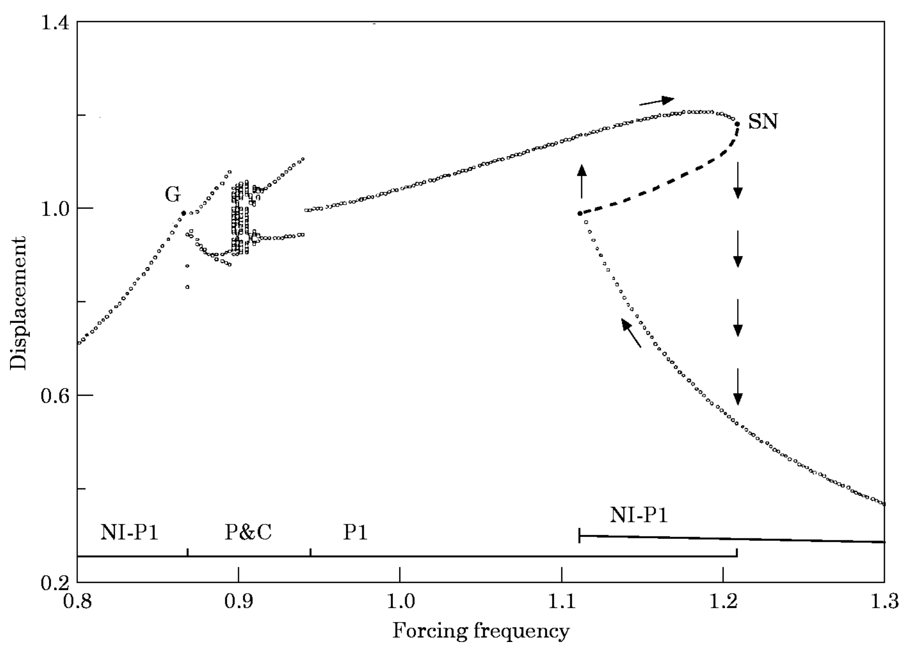

Figure 1. Bifurcation diagram for $c = 0{\cdot}1$, $f = 0{\cdot}26$, $r = 0{\cdot}2$ with the variation of ω from 0·8 to 1·3, where G indicates the point of grazing bifurcation, SN the saddle–node bifurcation, and the arrows indicate how the system would evolve as the parameter ω varies through the bifurcation points. The label NI-P1 denotes a period-1 non-impacting motion, P&C denotes periodic and chaotic impacting motions, and P1 a period-1 impacting motion.

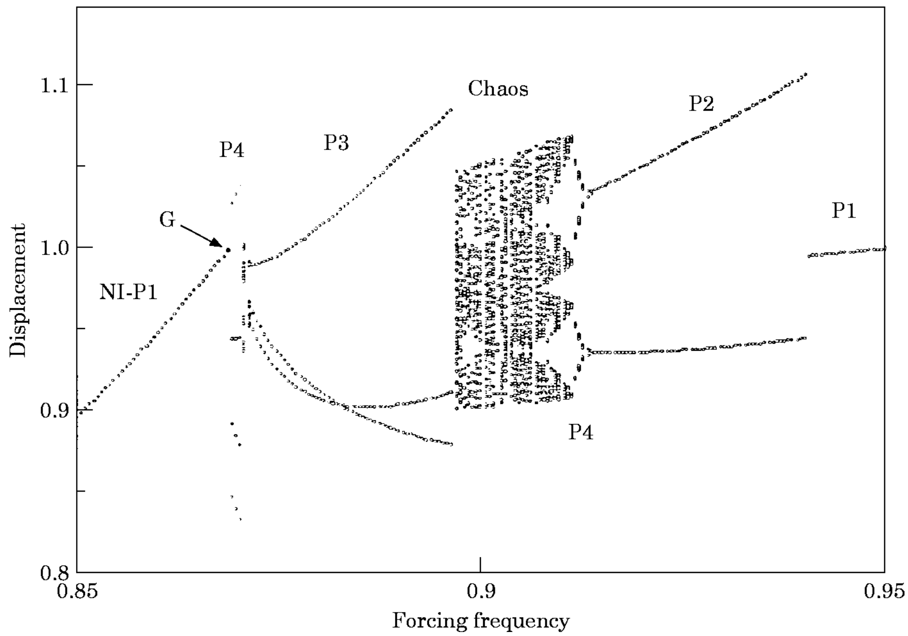

Figure 2. A close-up view of the bifurcation diagram within the parameter range $0{\cdot}85 < \omega < 0{\cdot}95$. The motions are indicated by the symbol P (periodic motion) followed by an integer which indicates the number of the forcing periods contained in an orbital period of the motion. G represents the grazing point.

Figure 2 displays a close-up view of the system response within the parameter range ($\omega = 0{\cdot}85$–$0{\cdot}95$). Different types of motion are marked by a symbol P followed by an integer which denotes the periodicity of the motion. For instance, P2 denotes a motion which repeats itself every two forcing periods. In the figure, apart from the non-impacting motion NI-P1 located within the range of $\omega < 0{\cdot}86885$, all other solutions are impacting motions such as the P4, P3, P2 and P1 located on the right side of G in Figure 2. Chaotic impacting motion occurs following the P3 motion and disappears with emergence of the P4 motion which itself evolves into an P2 motion after an inverse period-doubling bifurcation. As the system passes from the NI-P1 motion to the P4 orbit a grazing bifurcation occurs (at G) which plays a crucial role in determining the subsequent response [17, 22, 23]. At the grazing point, the map of the system is continuous but not differentiable (a singularity in the Jacobian of the map), and one of the eigenvalues of the Jacobian may be infinite [19]. The stable NI-P1 orbit becomes an unstable P1 orbit after the grazing point, the existence of which has been verified using analytical methods [18, 19].

The pattern of impacting motions close to the grazing point is complicated and sensitive to small changes in the parameter. To illustrate this, Figure 3 explores a finer view to reveal the detailed structure of the solution paths between the P4 and P3 orbits of Figure 2. In Figure 3(a), one can see the family of bifurcatons leading to a series of impacting motions: P4→P16→P12→P8→P4→chaos→P6→P3. Qualitative changes in these motions are due to further bifurcations, including grazing impacts, as the forcing frequency increases. The grazing impacts, as before, produce new higher order impacting orbits with different numbers of impacts during an orbital period of the solution, shown in Figure 3b. The overall effect of each of these further grazing bifurcations is not so severe as the grazing at G but these have not been investigated in detail here. In the figure one can see a transition P4→P16→P12→P8→P4, within a very narrow parameter regime ($\omega \approx 0{\cdot}87$–$0{\cdot}8705$) close to the grazing point G at $\omega_c \approx 0{\cdot}86885$. Numerical results indicate that this is a cascade of reverse period-adding bifurcations and the periodicity of the orbits after each bifurcation changes by the base of four. Individually, observing any branch of the bifurcation cascade, shows that the number of paths decreases by one through each

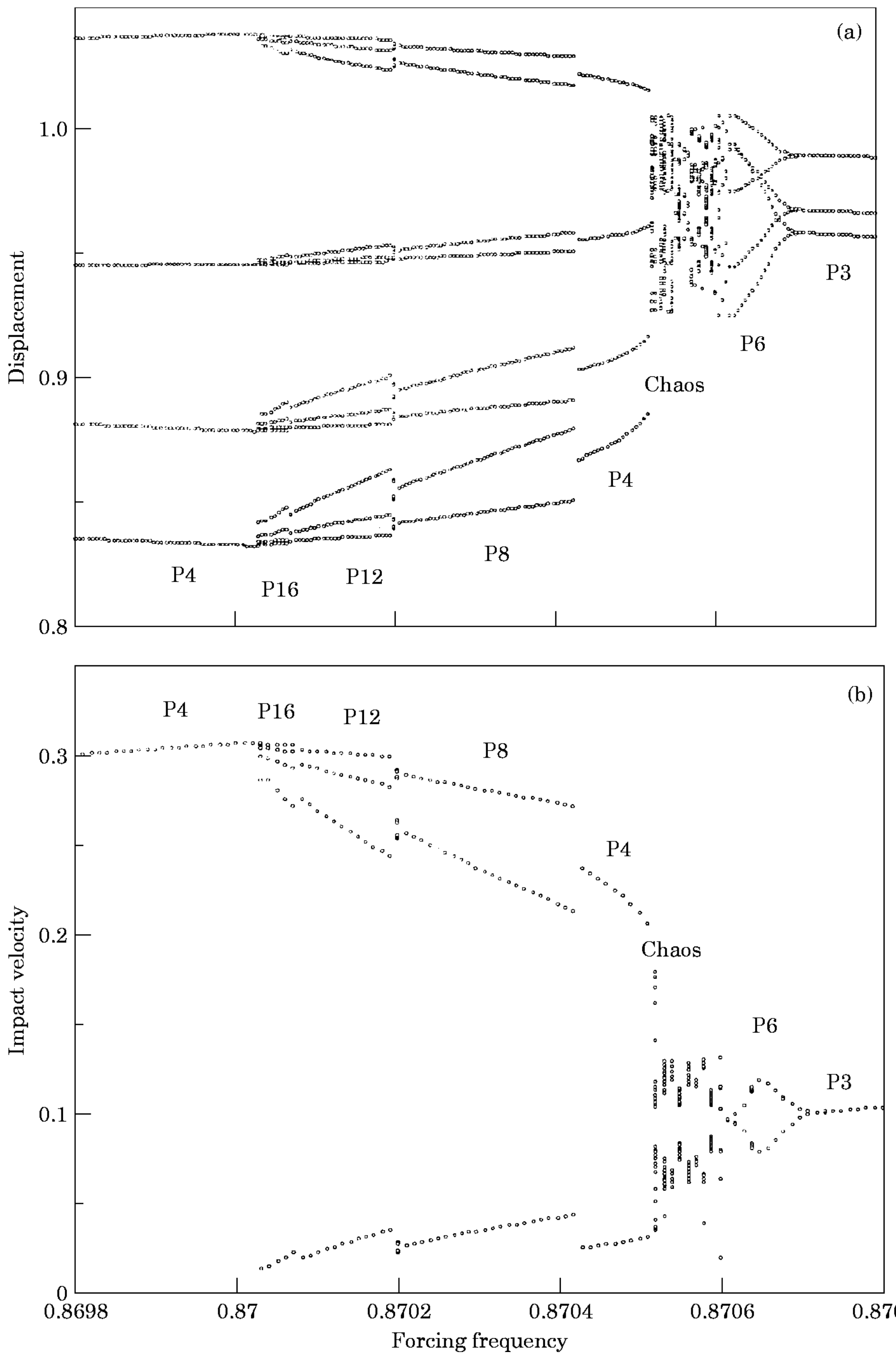

Figure 3. (a) A finer view of a group of higher periodic and chaotic impacting motions in the range of $0{\cdot}8698 < \omega < 0{\cdot}8708$. (b) Impact velocity, just before impact occurs, showing the number of impacts for the different impacting motions.

bifurcation. The scenario of this bifurcation pattern is very similar to the Nordmark map studied by Chin *et al*. [23] in which this typical phenomenon is regarded as a universal property for the impacting systems. In Figure 3(b) the P4 orbit ($\omega \approx 0{\cdot}86885$–$0{\cdot}87$) with one impact during an orbital period differs from the P4 orbit ($\omega \approx 0{\cdot}87043$–$0{\cdot}87052$) which has two impacts per orbital period (four forcing periods). It is clear that the P16 orbit has five impacts per orbital period and subsequently the number of impacts for the orbits reduces by one through each bifurcation. In Figure 3(b) the P3 and P6 orbits have one and two impacts respectively.

The bifurcation diagrams (Figures 1, 2 and 3) confirm the analytical prediction that there is no stable P1 orbit in the parameter regime ($\omega \approx 0{\cdot}86885$–$0{\cdot}94$) within which chaotic impacting motions occupy a relatively large portion. Close to the grazing point G, higher periodic orbits and chaotic orbits with larger number of impacts appear. The P4 orbit with one impact per orbital period is the stable orbit nearest to the grazing point G but this orbit has a relatively large impact velocity compared with other solutions. As stated, large impact velocities may cause excessive loads accelerating wear or resulting in structural damage.

4. TRACKING LOWER PERIODIC IMPACTING ORBITS

The goal of this study is to eliminate the complicated impacting motions that occur during a variation of the parameters (e.g., forcing frequency) close to the grazing bifurcation (such operations are common in engineering systems during start-up or shut-down procedures). In particular, a tracking control technique is applied to extend lower periodic impacting motions towards the grazing bifurcation for the parameter range where these orbits are initially stable but then become unstable such that (uncontrolled) higher periodic or chaotic impacting motions dominate the system performance. An unstable periodic impacting orbit stabilized near grazing has lower impact velocity which can greatly reduce the impact force. Thus the use of control leads to certain advantages of longer fatigue life, less wear and noise etc., under engineering considerations.

The use of newly developed control techniques [26–29, 35–39] can change the behaviour of the system either to specifically enhance the response, or in this case, to avoid the complicated impacting motions improving the system performance. Conceivably any one of these control measures (or other suitable methods) might be applied in conjunction with tracking techniques [28] which can extend a selected motion from the initially stable state to an unstable state through the parameter regimes where complicated impacting motions govern the system response. By so doing, the system behaviour can be greatly altered displaying a desired response over almost all the parameter range.

Here, to carry out the control, a so-called self-locating control scheme [26, 37] is used. This method is based on the Newton root finding algorithm and utilizes the feedback of an output sequence on accessible parameters. Before the control only an approximate location of the desired periodic orbit is required which can subsequently be automatically and accurately detected in the control process. Because of the self-locating function, the control method can be applied to track a periodic orbit with the variation of the parameter. In this particular application, the amplitude of the driving force f is taken as an accessible control parameter and, for completeness, some details are given below.

Consider an n-dimensional map, which may be written in the general form

$$\mathbf{x}_{i+1} = \mathbf{f}(\mathbf{x}_i, \mathbf{p}), \qquad \mathbf{x} \in \Re^n, \qquad \mathbf{p} \in \Re^l, \tag{2}$$

where $\mathbf{x}_i$ is an $n \times 1$ vector and $\mathbf{p}$ is an accessible system parameter vector which may be perturbed within a limiting range $\mathbf{p} \in (\mathbf{p}^* - \Delta\mathbf{p}, \mathbf{p}^* + \Delta\mathbf{p})$, with $\mathbf{p}^*$ the nominal value at which the system $\mathbf{f}$ is currently placed and where $\Delta\mathbf{p}$ is the maximum possible perturbation.

Suppose that only an approximate region is known within which lies an unstable periodic orbit $\mathbf{x}^*$ which is to be stabilized. To accurately locate this periodic solution, consider the residual map $\mathbf{\Phi}(\mathbf{x})$,

$$\mathbf{\Phi}(\mathbf{x}) = \mathbf{F}(\mathbf{x}, \mathbf{p}^*) - \mathbf{x}, \qquad \mathbf{F}(\mathbf{x}, \mathbf{p}^*) = \mathbf{f}^m(\mathbf{x}, \mathbf{p}^*), \tag{3}$$

where $\mathbf{f}(\mathbf{x}, \mathbf{p}^*)$ denotes the m-th iterate of $\mathbf{f}$. A period-m orbit $\mathbf{x}^*$ of the map $\mathbf{f}$ corresponds to one of the solutions of

$$\Phi(\mathbf{x}^*) = 0. \tag{4}$$

Upon starting from a point $\boldsymbol{x}_k$ in the neighbourhood of the unknown periodic orbit $\boldsymbol{x}^*$, this initial estimate of solution $\mathbf{x}^*$ is improved by using the Newton root finding algorithm,

$$\bar{\mathbf{x}}_{k+1} = \mathbf{x}_k - [\mathrm{d}\mathbf{\Phi}(\mathbf{x}_k)/\mathrm{d}\mathbf{x}]^{-1} \cdot \Phi(\mathbf{x}_k) = \mathbf{x}_k - [\mathbf{D}_k - \mathbf{I}]^{-1}(\mathbf{F}(\mathbf{x}_k, \mathbf{p}^*) - \mathbf{x}_k) \tag{5}$$

where $\mathbf{D}_k$ is the Jacobian matrix estimated at $\mathbf{x}_k$ provided that $[\mathbf{D} - \mathbf{I}]$ is not singular. Here $\bar{\mathbf{x}}_{k+1}$ is the new prediction of the solution $\mathbf{x}^*$. Provided that the system $\mathbf{F}$ can be adjusted from the state $\mathbf{x}_k$ to the new state $\bar{\boldsymbol{x}}_{k+1}$ (i.e., let $\boldsymbol{x}_{k+1} = \bar{\mathbf{x}}_{k+1}$), then iterating the process (5) results in convergence to the solution $\mathbf{x}^*$.

We control the system $\mathbf{F}$ from $\mathbf{x}_k$ to $\bar{\mathbf{x}}_{k+1}$ by means of a perturbation $\delta\mathbf{p}_k$ of the parameter $\mathbf{p}$ so that

$$\bar{\mathbf{x}}_{k+1} = \mathbf{F}(\mathbf{x}_k, \mathbf{p}^*) + \mathbf{G}_\mathbf{k}\delta\mathbf{p}_k, \qquad \mathbf{G}_k = (\partial\mathbf{F}(\mathbf{x}_k, \mathbf{p}^*)/\partial\mathbf{p}), \qquad \delta\mathbf{p}_k = (\mathbf{p}_k - \mathbf{p}^*). \tag{6}$$

Substituting expression (6) into equation (5) yields the perturbation $\delta\boldsymbol{p}_k$ of the parameter $\mathbf{p}$ as

$$\delta\mathbf{p}_k = -(\mathbf{G}_k^T\mathbf{G}_k)^{-1}\mathbf{G}_k^T([\mathbf{D}_k - \mathbf{I}]^{-1} + \mathbf{I})\,(\mathbf{F}(\mathbf{x}_k, \mathbf{p}^*) - \mathbf{x}_k). \tag{7}$$

Introducing the input $\mathbf{p}_k = \mathbf{p}^* + \delta\mathbf{p}_k$ into the system (2) during the time from k to $k+1$ forces the system from $\mathbf{x}_k$ to $\bar{\mathbf{x}}_{k+1}$. In the next control step, starting from $\mathbf{x}_{k+1}(\mathbf{x}_{k+1} = \bar{\mathbf{x}}_{k+1})$, $\delta\mathbf{p}_{k+1}$ may be calculated by (7) and $\mathbf{p}_{k+1} = \mathbf{p}^* + \delta\mathbf{p}_{k+1}$ fed into the system (2) and so on. Continued iteration of this control process eventually brings the system onto the periodic orbit $\boldsymbol{x}^*$ provided that the initial $\mathbf{x}_k$ is sufficiently close to the solution $\mathbf{x}^*$. With this *caveat* satisfied, convergence is rapid following the "quadratic convergence" property of the Newton method. No special account is taken of any grazing events during the control process. The control method is based on a continuous map and therefore, despite the discontinuity in the derivative of the mapping at G, the scheme is successful. Of course it may be that although if one follows a stable path grazing bifurcations will occur, the unstable path itself remains unaffected.

The control signal is renewed once during each period of the tracked orbit. Considered here are three lower periodic impact orbits (P1, P2 and P3) and these are extended towards the grazing point G in place of the stable higher periodic and chaotic impacts orbits which would naturally exist.

Figure 4 demonstrates the loci of the stabilized P1, P2 and P3 orbits by plotting the maximum displacement of the orbit during an orbital period. These impact orbits have only one impact for each orbit period, as can be seen from the inset phase portraits of the various solutions given in Figure 4. Each tracking process starts from the state where the orbit to be tracked is stable. Even before the system decays onto the stable orbit, the use of the self-locating control can accelerate the convergence and reduce the transient time to reach the steady state. In a tracking process, the parameter ω varies once the difference

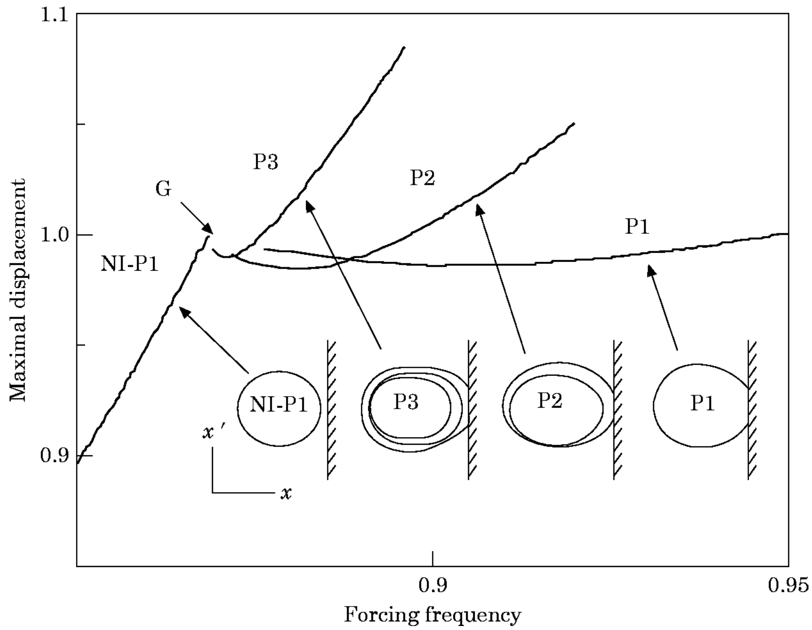

Figure 4. The tracked lower periodic impacting motions (P1, P2 and P3) extended towards the grazing point G as the parameter ω decreases. The orbital pattern of the impacting motions is indicated in the phase space $(x, \dot{x})$.

of amplitudes of the stabilized orbit, during an orbital period, is within a required precision of $\Delta\omega = 0{\cdot}0001$. This parameter varying step should be very small particularly when the stabilized orbit approaches the grazing point where the eigenvalue of the orbit becomes infinitely large. As can be seen, the P1 and P2 impact orbits can be stabilized and extended through the regime ($\omega \approx 0{\cdot}897$–$0{\cdot}91$) in which chaotic impacting motions originally dominate the system performance (see Figure 2). The P3 orbit can be stabilized even up to a very close distance from the grazing point and certainly extended through the regime of the higher periodic and chaotic impacting motions which initially govern the system. However, there is a limit for stabilisation of each orbit close to the grazing point. The P1 impact orbit can be extended close to the grazing point ($\omega_c \approx 0{\cdot}86885$) up to $\omega > 0{\cdot}8762$ and for the P2 orbit up to $\omega > 0{\cdot}872$ while the P3 orbit can be stabilized to $\omega > 0{\cdot}8695$ by using the self-locating method; see Figure 4.

The variations of the eigenvalues of the stabilized P1, P2 and P3 orbits during the tracking process are shown in Figure 5. As the parameter ω decreases, the absolute value of the eigenvalue increases. Close to the grazing point, the values of the eigenvalue of these three orbits increase dramatically. Theoretical studies [16, 22, 34] verified that the eigenvalue of the unstable impact orbits become infinitely large at the grazing point because of the singularity of the Jacobian of the map. An orbit with large eigenvalues is very sensitive to any error which makes control difficult [39]. Figure 5 indicates that the P3 orbit can be stabilized closer to the grazing point than can the P1 and P2 orbits. The three cases exhibit a common feature that, just before the failure in the tracking of each orbit, the eigenvalue of the orbit increases rapidly. Any tiny change of the parameter ω gives rise to a large change of the eigenvalue such that control cannot extend the stabilized orbit further. The value of the parameter ω corresponding to a rapid increase of eigenvalues can be seen as a threshold at which control fails.

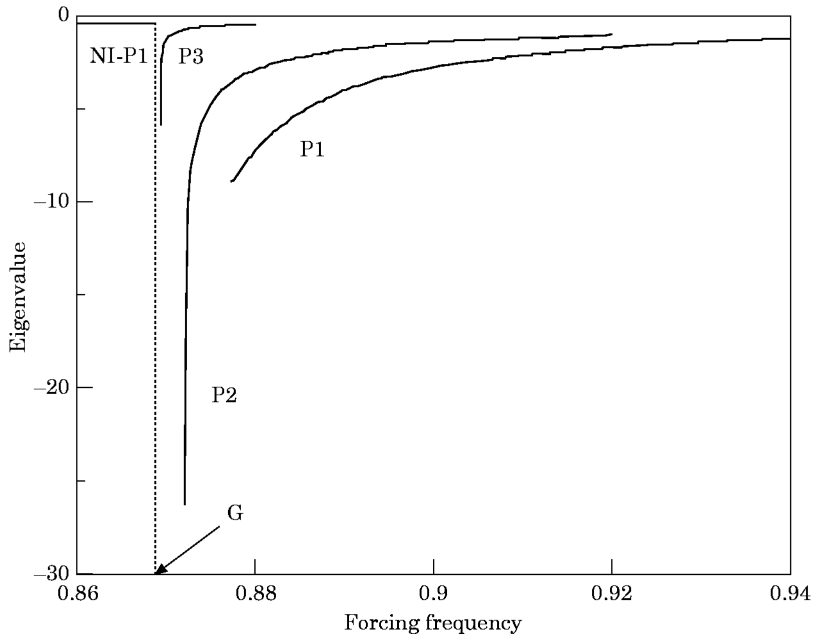

Figure 5. The largest (absolute value) eigenvalue of the impacting motions (P1, P2 and P3).

Figure 6 shows the velocity of impact for each stabilized orbit in the domain of the tracked orbits. It is apparent that the impact velocity decreases as the stabilized orbit approaches the grazing point at $\omega_c \approx 0{\cdot}86885$. In this figure, the P1 impact orbit is naturally stable at $\omega = 0{\cdot}95$ where the impact velocity of the orbit is approximately 0·4. This orbit becomes unstable as $\omega < 0{\cdot}94$ and can be stabilized towards the grazing point

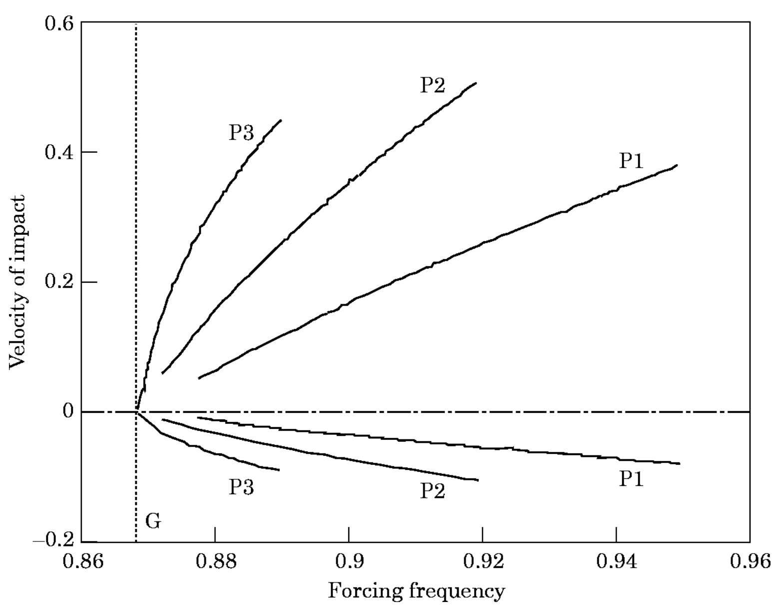

Figure 6. The impact velocity of the stabilized impacting motions. The solid lines above and below the zero broken line (horizontal) respectively indicate the velocity just before and after impact occurs. The vertical broken line indicates the value of ω corresponding to the grazing point.

at $\omega = 0{\cdot}8762$ where the impact velocity of the P1 orbit is about 0·05. Reductions in velocity of impact occur for the P2 and P3 orbits though a rigorous scaling has not been established (see reference [34]). In particular, the impact velocity for the stabilized P3 orbit almost reaches zero. It is known that impact velocity governs impact force which is of much concern in engineering, and it has been shown that applying control can significantly decrease the impact velocity in a systematic way.

4. CONCLUSIONS

The behaviour of a simple impacting beam with periodic excitation can be very complicated, particularly in the regime where grazing bifurcations occur. Grazing bifurcations can produce high periodic and chaotic impacting motions with relatively large impact velocity and various numbers of impacts per orbital period of the solution. Such motions can cause higher impact forces leading to excessive loads, wear, or unacceptable noise.

The aim of this research was to use techniques developed for the control of chaos to eliminate any high periodic and chaotic impacting motions. Numerical evidence has been shown that the self-locating method of control can achieve this goal. This method has been applied to track lower periodic impacting motions towards the regime where the high periodic and chaotic impacting motions naturally exist (i.e., are stable solutions) and dominate the performance of the system. The lower periodic impacting motions stabilized near the grazing incidence have much lower impact velocities resulting in a reduction of the impact force. These advantages may be of wider interest in engineering.

REFERENCES

1. V. I. Babitsky 1976 *The Theory of Vibro-Impact Systems* (in Russian). Nauka: Moscow.
2. Yu. I. Neimark and P. S. Landa 1992 *Stochastic and Chaotic Oscillations*. Dordrecht: Kluwer.
3. P. S. Landa 1996 *Nonlinear Oscillations and Waves in Dynamical Systems*. Dordrecht: Kluwer.
4. F. Peterka and J. Vacik 1992 *Journal of Sound and Vibration* **154,** 95–115. Transition to chaotic motion in mechanical systems with impacts.
5. S. W. Shaw and P. J. Holmes 1983 *Journal of Sound and Vibration* **90,** 129–155. A periodically forced piecewise linear oscillator.
6. S. W. Shaw and P. J. Holmes 1983 *Physical Review Letters* **51**, 623–626. Periodically forced impact oscillator.
7. S. W. Shaw 1985 *Journal Applied Mechanics* **52**, 453–458. Dynamics of harmonically excited systems having rigid amplitude constraints, Part I: Subharmonic motions and local bifurcations.
8. S. W. Shaw 1985 *Journal Applied Mechanics* **52**, 459–464. Dynamics of harmonically excited systems having rigid amplitude constraints, Part II: Chaotic motions and global bifurcations.
9. F. Pfeiffr and A. Kunert 1990 *Nonlinear Dynamics* **1**, 63–74. Rattling models from deterministic to stochastic processes.
10. P. C. Tung and S. W. Shaw 1988 *Journal of Vibration and Acoustics Stress Reliability Design* **110**, 193–200. The dynamics of an impact print hammer.
11. G. S. Whiston 1987 *Journal of Sound and Vibration* **115**, 303–319. The vibro-impact response of a harmonically excited and preloaded one dimensional linear oscillator.
12. G. S. Whiston 1987 *Journal of Sound and Vibration* **118**, 395–429. Global dynamics of a vibro impact linear oscillator.
13. M. Sharif-Bakhtiar and S. W. Shaw 1988 *Journal of Sound and Vibration* **126**, 221–235. The dynamic response of a centrifugal pendulum vibration absorber with motion-limiting stops.
14. J. F. Deck and S. Dubowsky 1992 *ASME Flexible Mechanisms*, *Dynamics and Analysis* **47**, 461–469. On the limitations of predictions of the dynamic response of machines with clearance connections.
15. J. M. T. Thompson, A. R. Bokaian and R. Ghaffari 1984 *Journal of Energy Resources*

Technology **106**, 191–198. Subharmonic and chaotic motions of compliant offshore structures and articulated mooring towers.
16. S. R. Bishop 1994 *Philosophical Transactions of the Royal Society of London* **347A**, 347–451. Impact oscillators.
17. S. Foale and S. R. Bishop 1992 *Philosophical Transactions of the Royal Society of London* **338A**, 547–556. Dynamical complexities of forced impact systems.
18. M. G. Thompson, S. R. Bishop and S. Foale 1994 *Machine Vibration* **3**, 10–17. An experimental study of low velocity impacts.
19. S. Foale and S. R. Bishop 1994 *Nonlinear Dynamics* **6**, 285–299. Bifurcations in impact oscillators.
20. C. J. Budd and F. Dux 1994 *Philosophical Transactions of the Royal Society of London A* **347**, 365–389. Chattering and related behaviour in impact oscillators.
21. S. J Hogan 1989 *Proc. Roy Soc. Lond. A* **425**, 441–476. On the dynamics of rigid-block motion under harmonic forcing.
22. A. B. Nordmark 1991 *Journal of Sound and Vibration* **145**, 279–297. Non-periodic motion caused by grazing incidence in an impact oscillator.
23. W. Chin, E. Ott, H. E. Nusse and C. Grebogi 1995 *Physics Letters A* **201**, 197–204. Universal behaviour of impact oscillators near grazing incidence.
24. J. Weger, D. Binks, J. Molenaar and W. van de Water 1996 *Physical Review Letters* **76**, 3951–3954. Generic behaviour of grazing impact oscillators.
25. S. R. Bishop, M. G. Thompson and S. Foale, 1996 *Proceedings of the Royal Society London. A* **452**, 2579–2592. Prediction of period-1 impacts in a driven beam.
26. D. Xu and S. R. Bishop 1996 *Physics Letters A* **210**, 273–278. Self-locating control of chaotic systems using a Newton algorithm.
27. E. Ott, C. Grebogi and J. A. Yorke 1990 *Physical Review Letters* **64**, 1196–1199. Controlling chaos.
28. I. B. Schwartz and I. Traindaf 1992 *Physical Review A* **46**, 7439–7444. Tracking unstable orbits in experiments.
29. J. Starret and R. Tagg 1995 *Physical Review Letters* **74**, 1974–1977. Control of a chaotic parametrically driven pendulum.
30. E. L. B. Van de Vorst, D. H. Van Campen and R. H. B. Fey 1996 *Journal of Sound and Vibration* **192**, 913–925. Periodic solutions of a multi-DOF beam system with impact.
31. S. Natsiavas 1990 *Journal of Sound and Vibration* **141**, 97–102. Stability and bifurcation analysis for oscillators with motion limiting constraints.
32. C. Budd, F. Dux and A. Cliffe 1995 *Journal of Sound and Vibration* **184**, 475–502. Effect of frequency and clearance variation on single degree-of-freedom oscillators.
33. C. Budd and F. Dux 1994 *Nonlinearity* **7**, 1191–1224. Intermittency in impact oscillators close to resonance.
34. H. Lamba and C. Budd 1994 *Physical Review E* **50** (1), 84–90. Scaling of Lyapunov exponents at non-smooth bifurcations.
35. D. Xu and S. R. Bishop 1994 *Chaos Solutions & Fractals* **4**, 1931–1942. Steering dynamical trajectories to target a desired state.
36. D. Xu and S. R. Bishop 1995 *International Journal of Bifurcation and Chaos* **5**, 1741–1748. A contraction-mapping-based control approach to stabilize chaotic systems.
37. S. R. Bishop and D. Xu 1996 *Journal of Sound and Vibration* **194**, 287–293. Stabilizing the parametrically excited pendulum onto high order periodic orbits.
38. S. R. Bishop, D. Xu and M. J. Clifford 1996 *Proceedings of the Royal Society London A* **452**, 1–18. Flexible control of the parametrically excited pendulum.
39. S. R. Bishop and D. Xu 1996 *Physical Review E* **54** (4), 3204–3210. Control of chaos in noisy flows.